HHS Public Access

Author manuscript

J Immunol. Author manuscript; available in PMC 2021 September 23.

Published in final edited form as:

J Immunol. 2020 May 01; 204(9): 2464–2473. doi:10.4049/jimmunol.1900430.

A Critical Role of Formyl Peptide Receptors in Host Defense against *Escherichia coli*

Meihua Zhang[*,†,1], **Ji-Liang Gao**[‡,1], **Keqiang Chen**[†], **Teizo Yoshimura**[§], **Weiwei Liang**[†,¶], **Wanghua Gong**[‖], **Xiaoqing Li**[†], **Jiaqiang Huang**[†], **David H. McDermott**[‡], **Philip M. Murphy**[‡], **Xietong Wang**[*], **Ji Ming Wang**[†]

[*]Key Laboratory of Birth Regulation and Control Technology of National Health Commission of China, Shandong Provincial Hospital Affiliated to Shandong University, Jinan 250002, People's Republic of China;

[†]Cancer and Inflammation Program, Center for Cancer Research, National Cancer Institute at Frederick, Frederick, MD 21702;

[‡]Laboratory of Molecular Immunology, National Institute of Allergy and Infectious Diseases, Bethesda, MD 20892;

[§]Department of Pathology and Experimental Medicine, Graduate School of Medicine, Dentistry and Pharmaceutical Sciences, Okayama University, Okayama 700-8558, Japan;

[¶]Department of Immunology, School of Basic Medical Sciences and Key Laboratory of Medical Immunology of Ministry of Health, Peking University Health Science Center, Beijing 100191, People's Republic of China;

[‖]Basic Research Program, Leidos Biomedical Research, Inc., Frederick, MD 21702

Abstract

Formyl peptide receptors (FPRs, mouse Fprs) belong to the G protein–coupled receptor superfamily and mediate phagocyte migration in response to bacteria- and host-derived chemoattractants; however, knowledge about their in vivo roles in bacterial pathogenesis is limited. In this study, we investigated the role of Fpr1 and Fpr2 in host defense against *Escherichia coli* infection. In vitro, we found that supernatants from *E. coli* cultures induced chemotaxis of wild-type (WT) mouse bone marrow–derived neutrophils and that the activity was significantly reduced in cells genetically deficient in either Fpr1 or Fpr2 and was almost absent in cells lacking both receptors. Consistent with this, *E. coli* supernatants induced chemotaxis and MAPK phosphorylation in HEK293 cells expressing either recombinant Fpr1 or Fpr2 but not untransfected parental cells. WT bone marrow –derived neutrophils could actively phagocytose

Address correspondence and reprint requests to Dr. Xietong Wang or Dr. Ji Ming Wang, Key Laboratory of Birth Regulation and Control Technology of National Health Commission of China, Shandong Provincial Hospital Affiliated to Shandong University, Jinan 250002, People's Republic of China (X.W.) or Cancer and Inflammation Program, Center for Cancer Research, National Cancer Institute at Frederick, Building 560, Room 31-76, 8560 Progress Drive, Frederick, MD 21702 (J.M.W.). wxt65@vip.163.com (X.W.) or wangji@mail.nih.gov (J.M.W.).

[1]M.Z. and J.-L.G. contributed equally to the study.

Disclosures

The authors have no financial conflicts of interest.

The online version of this article contains supplemental material.

and kill *E. coli*, whereas both activities were diminished in cells lacking Fpr1 or Fpr2; again, an additive effect was observed in cells lacking both receptors. In vivo, Fpr1 and Fpr2 deficiency resulted in reduced recruitment of neutrophils in the liver and peritoneal cavity of mice infected with inactivated *E. coli*. Moreover, *Fpr1*$^{-/-}$ and *Fpr2*$^{-/-}$ mice had significantly increased mortality compared with WT mice after i.p. challenge with a virulent *E. coli* clinical isolate. These results indicate a critical role of Fprs in host defense against *E. coli* infection.

Escherichia coli, which belongs to the family of *Enter-obacteriaceae*, is harmless under homeostatic conditions and benefits the hosts by producing vitamin K2 (1), essential for physiological coagulation. However, *E. coli* causes opportunistic infections in immunosuppressed subjects with a high mortality rate, indicating that resistance to opportunistic *E. coli* infection depends on immune responses.

Activation of innate immune cells through pattern recognition receptors (PRRs), such as TLRs and Nod-like receptors, is important for antibacterial host responses (2). Among TLRs, TLR4 recognizes LPS released by Gram-negative bacteria, including *E. coli* (3, 4). TLR4 activation enhances the phagocytic capacity of neutrophils and monocyte-macrophages in bacterial infection (5, 6). TLR4 is also involved in promoting immune cell recruitment, which is not mediated by its chemotactic activity, but rather, by indirectly upregulating the production of chemoattractants that activate G protein–coupled receptors (GPCRs) expressed on immune cells.

Formyl peptide receptors (FPRs in humans, Fprs in mice) belong to the chemoattractant GPCR family and are considered atypical PRRs. They were originally identified based on their capacity to recognize *N*-formyl peptides produced in nature by degradation of either bacterial (e.g., *E. coli*) (7–10) or host cell mitochondrial proteins, which are proinflammatory products liberated after cell damage (11, 12). FPRs (mouse Fprs), in particular FPR2 (Fpr2), have been shown to also recognize a variety of host-derived nonformylated peptide ligands associated with inflammatory responses and cancer, implicating their involvement in multiple pathophysiological conditions (9, 13). FPRs have been shown to play an essential role in host resistance to *Listeria* infection by mediating a rapid neutrophil infiltration in infected mouse organ (14, 15). This first wave of neutrophil recruitment precedes the production of chemokines induced by *Listeria* lipoproteins that activate TLR2. Thus, Fprs represent the front line of host response to *Listeria* infection.

However, despite the fact that *E. coli*–derived formylated peptides were the first chemotactic agonists identified for FPRs, the role of these receptors in host responses to *E. coli* infection has not been defined. In this study, we fill this gap using genetically engineered mice deficient in Fpr family members 1 or 2.

Materials and Methods

Animals and reagents

Mouse strains deficient in Fpr1 (*Fpr1*$^{-/-}$) or Fpr2 (*Fpr2*$^{-/-}$) were generated as described (15, 16). Fpr1/2 double deficient mice were generated by replacing a 7-kb fragment containing exon 1 of the Fpr1 gene as well as the promoter regions of Fpr1 and 2 genes with a neo gene

cassette to construct a targeting vector. The neo gene was subsequently deleted by crossing with β-actin Cre–transgenic mice. Mice were backcrossed to C57BL/6 mice (Charles River, Frederick, MD) for at least eight generations before use. All mice were housed in the animal facility at Frederick National Laboratory for Cancer Research and were used at 8–12 wk of age. Mouse experiments were approved by Animal Care and Use Committee of the National Cancer Institute and the National Institute of Allergy and Infectious Diseases and performed in accordance with the procedures outlined in the "Guide for Care and Use of Laboratory Animals" (National Research Council, 1996, National Academy Press, Washington, D.C.).

Rat anti-mouse Ly6G and 6-diamidino-2-phenylindole Abs were obtained from Becton-Dickinson (Franklin Lakes, NJ); goat anti-Rat Ig-FITC Abs were obtained from eBioscience (San Diego, CA); Amplex Red Hydrogen Peroxide/Peroxidase Assay Kit was from Invitrogen (Eugene, OR); rat anti-mouse Abs against p-p38 MAPK (Thr^{180}/Tyr^{182}), p38, p-ERK1/2 (Thr^{202}/Tyr^{204}), ERK1/2, pAkt, Akt, IkBα, GAPDH, and HRP-linked anti-rabbit IgG Abs were from Cell Signaling Technology (Beverly, MA); FITC isomer 1 and poly-lysine were from Sigma-Aldrich (St. Louis, MO); Boc-MLF, WRW4, Boc-2, fMLF, and SDF1α (CXCL12) were from Tocris (Ellisville, MO); the p38 inhibitor SB203580, ERK1/2 inhibitor PD98059, Akt inhibitor Mk2206, and IκB inhibitor PDTC were from Abcam (Cambridge, MA); Microbial DNA Isolation Kit was from Thermo Fisher Scientific (Waltham, MA); DNeasy UltraClean Microbial Kit was from Qiagen (Germantown, MD).

Isolation of mouse neutrophils

Mouse bone marrow (BM) was collected and treated with ACK lysing buffer (Quality Biological, Gaithersburg, MD) after centrifugation. The cells were suspended in PBS, filtered through a 40-μm filter, and then suspended in RPMI 1640 medium containing G-CSF (10 ng/ml; Thermo Fisher Scientific), 10% heat-inactivated FCS, and 2% penicillin and streptomycin. After a 24-h culture, cells were collected and smeared on slides coated with poly-lysine (Sigma-Aldrich) for characterization. The cells were fixed in 4% neutrally buffered formalin for 15 min and stained with primary Abs (anti-mouse Ly6G, 1:100) followed by goat anti-rabbit Ig-FITC (1:1000). DAPI was used to stain nuclei.

Isolation of *E. coli* from the mucosa of mouse colon

E. coli adhered to mouse colon epithelium was isolated by scraping the mucosa and culturing in LB Broth (Gibco) agar at 37°C, 180 rpm, for 48 h. Then, 50 μl of bacterial culture medium was used for aerobic incubation in Violet Red Bile Lactose Agar for 24 h. Single-bacterial colonies were used to extract DNA for PCR expansion and 16S rRNA sequencing. DNA was extracted by using a DNeasy UltraClean Microbial Kit (Qiagen). Amplification was performed in a PCR Sprint Thermocycler (Hybaid; Thermoelectron, Waltman, MA). Primers, with forward sequence 5′-TG GCTCAGGACGAACGCTGGCGGC-3′ and reverse sequence 5′-CCTACTGCTGCCTCCCGTAGGAGT-3′ (Integrated DNA Technologies, Skokie, IL), were used for *E. coli* identification. The amplification conditions were 5 min at 95°C, 30 cycles of 95°C for 45 s, 58°C for 1 min, and 72°C for 45 s, and a final extension at 72°C for 10 min. PCR products were resolved on 1.5% agarose gel by electrophoresis and visualized after ethidium bromide staining. 16S rRNA sequencing were performed by Animal Molecular

Diagnostics Laboratory, Leidos Biomedical Research. The results of the sequencing were verified with those in the GenBank database by using the Basic Local Alignment Search Tool (BLAST) program (17). *E. coli* used for functional assays in this study was not opsonized.

Chemotaxis assays

The chemotaxis of neutrophils and HEK293 cells was examined by using polycarbonate membranes with 5-μm (neutrophils) or 8-μm pore size (HEK293 cells) in 48-well chambers. Deactivated *E. coli* was prepared by incubating the bacteria at 65°C for 30 min, and the supernatant was collected. *E. coli* supernatant (30 μl) in different dilutions were placed in the lower wells of the chamber, and 50 μl of cells (5×10^6/ml for neutrophils and 5×10^5/ml for HEK293 cells) suspended in RPMI 1640 with 0.5% BSA were placed in the upper wells. After incubation at 37°C (neutrophils for 90 min, HEK293 cells for 210 min), the membranes were washed, fixed, and stained with Diff-Quik. Migrating cells were counted under microscopy at ×400 magnification in three random fields. In experiments with Fpr antagonists, neutrophils were incubated with Fpr1 antagonist Boc-MLF (5 μg/ml), Fpr2 antagonist WRW4 (10 μg/ml), and Boc-MLF (5 μg/ml) + WRW4 (10 μg/ml) for 30 min and then added to the upper wells of the chemotaxis chamber.

Phosphorylation of MAPKs

The capacity of *E. coli* to activate MAPK and IkBα via Fpr1 and Fpr2 was detected by Western blotting. HEK293 cells (5×10^5 cells/ml) transfected with Fpr1 or Fpr2 were incubated in serum-free DMEM medium overnight and 40 μl/ml of *E. coli* supernatant (from 5×10^8 bacteria per milliliter) were added for 5 and 10 min to measure p-p38, ERK1/2, AKT, and IkBα.

Neutrophil phagocytosis and killing of *E. coli*

Mouse neutrophils were exposed to *E. coli* at a ratio of 1:10 (polymorphonuclear neutrophil [PMN]/bacteria) suspended in 1 ml of cell culture medium without antibiotics. After different times (15, 30, 45, and 60 min) at 37°C, the cells were extensively washed with sterile PBS, lysed in 0.1% Triton X-100 in H_2O, plated on LB agar plates, and incubated at 37°C overnight. CFUs were then counted.

H_2O_2 release

The experiments were performed according to the protocol of Amplex Red Hydrogen Peroxide/Peroxidase Assay Kit (Invitrogen). Mouse neutrophils (1×10^6 cells per milliliter) were cocultured with 10-fold live *E. coli* in RPMI 1640 medium containing 10% FCS at 37°C. A microplate reader was used for measurement of absorbance at ~560 nm. In culture groups with Fpr antagonists, the cells were incubated with Boc-MLF (5 μg/ml), WRW4 (10 μg/ml), or BOC_2 (10 μg/ml) for 30 min before measurement.

Neutrophil recruitment by *E. coli* in vivo

Mice were i.v. injected with *E. coli* (5×10^4 in 100 μl of PBS) through the tail vein, then were euthanized at 4 h after injection. Mouse livers were harvested, fixed in 10% formalin,

paraffin imbedded, sectioned in 5-μm slides, stained with H&E, then observed under light microscopy. Neutrophil aggregates in the liver was photographed and cell number was enumerated under microscopy at ×200 and ×1000 magnifications.

Heat-deactivated *E. coli* (5×10^5 in 100 μl of PBS) labeled with FITC were also injected into mouse peritoneal cavity to elicit neutrophil exudation. Mice were euthanized at different times after the injection and neutrophils were collected by washing the peritoneal cavity with 5 ml of ice-cold PBS. The cells were then labeled with the neutrophil-specific Ab Ly6G and counted by flow cytometry. Cxcl1 and Cxcl2 in the peritoneal exudate were measured by using U-PLEX Biomarker Group 1 (mouse) multiplex assays (courtesy of Ms. Yanyu Wang, Leidos Biomedical Research; MSD, Rockville, MD).

Challenge of Fpr1$^{-/-}$ mice with a virulent *E. coli* clinical isolate

A virulent *E. coli* clinical isolate obtained from patient blood at the National Institutes of Health Clinical Center was used for this experiment. *E. coli* was grown to log-phase in LB Broth, aliquoted in 1-ml volumes, and stored at −70°C. For each experiment, a vial of bacteria was thawed and diluted in PBS. For the mortality assay, we first established the LD_{50} for wild-type (WT) control C57BL/6 mice, which was ~10^6 CFUs via i.p. infection. Using the LD_{50} dose, we infected 6- to 8-wk-old littermates of *Fpr1*$^{+/+}$ and *Fpr1*$^{-/-}$ mice. For the bacterial burden and in vivo neutrophil recruitment assay, mice were infected with 3×10^6 bacteria i.p. and euthanized 3 h postinfection. Then, the peritoneal cavity was washed with 10 ml of PBS, and the number of viable *E. coli* were determined by plating on LB agar plates, the number of leukocytes were determined by hemocytometer, and the percentages of neutrophils among the recruited cells were determined by H&E staining.

Statistical analyses

All experiments were performed at least three times with similar results. Data are presented as the mean ± SEM. Statistical analysis was performed by using two-tailed Student *t* test. A *p* value <0.05 was considered statistically significant.

Results

Characterization of mouse neutrophils and *E. coli*

Neutrophils were isolated from WT mouse BM after culture with G-CSF for 24 h. The cells were labeled with the neutrophil-specific Ab Ly6G and showed more than 85% purity (Fig. 1A, 1B). Neutrophils obtained from Fpr single or double deficient mice exhibited morphology comparable with the cells from WT mice. We also isolated bacteria from colon mucosa of WT C57BL/6 mice treated with DSS in drinking water for 5 d. Diff-Quik staining showed that the bacteria were rod-like (Fig. 1C) and Gram-negative (Fig. 1D). *E. coli*–specific primers were used to amplify bacterial DNA by PCR that confirmed the colony as *E. coli* (Fig. 1E).

Involvement of Fprs in sensing *E. coli*–derived chemotactic signals

We then examined the capacity of Fprs as mediators of host defense to recognize *E. coli*. Supernatants from *E. coli*–induced migration of neutrophils isolated from the BM of WT

mice. Use of Fpr antagonists revealed that the chemotactic activity of *E. coli* supernatant for neutrophils was dependent on Fprs because either Fpr1 or Fpr2 antagonist was able to reduce neutrophil migration, and a combination of both Fpr1 and Fpr2 antagonists almost completely abolished neutrophil chemotaxis induced by the *E. coli* supernatant (Fig. 2A). To verify the requirement of Fprs for *E. coli* supernatant–induced chemotaxis of mouse neutrophils, we used cells isolated from BM of mice deficient in Fpr1, Fpr2, or both. Fig. 2B, 2C show that the chemotactic activity of both an *E. coli*–derived chemotactic peptide fMLF and the bacterial supernatant was significantly reduced for neutrophils isolated from either Fpr1- or Fpr2-deficient mice, and the activity was almost completely absent for cells isolated from mice deficient in both Fpr1 and Fpr2. Therefore, Fpr1 and 2 mediate migration of mouse neutrophils to *E. coli*–derived chemoattractants. We further used gain of function criteria with HEK293 cells transfected to express Fpr1 or Fpr2 to ascertain the receptor interaction with *E. coli* chemoattractants. As shown in Fig. 2D, parental HEK293 did not show any chemotactic response to *E. coli* supernatant. In contrast, HEK293 cells expressing Fpr1 or Fpr2 each demonstrated potent chemotaxis in response to *E. coli* supernatant. Therefore, the results obtained with neutrophils deficient in Fprs and HEK293 genetically engineered to express Fprs all unequivocally demonstrate the involvement of Fprs in mediating the chemotactic activity derived from *E. coli*.

We further examined the capacity of Fprs to mediate the phosphorylation of MAPKs and Akt, which have been implicated in cell activation by chemotactic antagonists. Fig. 3A, 3B show that both Fpr1- and Fpr2-transfected HEK293 cells were activated by *E. coli* supernatant with rapid phosphorylation of p38 and ERK1/2 MAPKs as well as Akt. The supernatant treatment of the cells also caused reduced cytoplasmic total IkBα as an indicator of NF-κB activation. The ability of Fprs to mediate neutrophil activation by *E. coli* supernatant was confirmed by inhibition of the cell response by inhibitors of MAPKs, Akt, and IkBα (Fig. 3C). These results indicate the capacity of Fprs to mediate a multitude of biological activities in cells expressing these receptors in response to *E. coli*–derived agonists.

Fpr-dependent *E. coli* phagocytosis and killing by neutrophils

We next investigated the capacity of Fprs to mediate endocytosis and killing of *E. coli* by neutrophils. We first cocultured WT mouse-derived neutrophils with *E. coli* for different time points, then lysed cells to detect phagocytosed bacteria. We found that the number of *E. coli* colonies from lysed WT mouse neutrophils reached a peak at 30 min after coculture with declination at 45 and 60 min, suggesting clearance of the bacteria (Fig. 4A, 4B). However, neutrophils from mice deficient in Fpr1 or Fpr2 exhibited significantly diminished phagocytosis of *E. coli* in cells, with a more prominent reduction in phagocytosis by cells deficient in both Fprs (Fig. 4A, 4B). In addition, neutrophils deficient in Fprs showed much slower clearance, as is most evident at 60 min after coculture with *E. coli* (Fig. 4B–D).

To clarify the mechanisms of neutrophil killing of *E. coli*, we examined the release of hydrogen peroxide (H_2O_2) by mouse neutrophils postinfection by *E. coli*. We observed that H_2O_2 released by WT neutrophils reached a peak at 30 min after *E. coli* infection and significantly decreased at 45 and 60 min. This release of H_2O_2 by WT neutrophils infected

with *E. coli* declined when the cells were pretreated with antagonists against Fpr1 or Fpr2 with an additive inhibition when the antagonist for both Fpr1 and Fpr2 was used (Fig. 5A). In addition, neutrophils derived from BM of mice deficient in either Fpr1 or Fpr2 showed decreased release of H_2O_2 after *E. coli* infection with further decrease in cells deficient in both receptors (Fig. 5B). Because H_2O_2 is essential for neutrophil elimination of invading pathogens, our results indicate the critical role of Fprs in mediating neutrophil capture and killing of *E. coli*.

We also have performed neutrophil extracellular trap (NET) assays with Fpr-deficient neutrophils (Supplemental Fig. 2), in which Fpr1 deficiency did not substantially affect the NET-forming capacity of neutrophils, whereas Fpr2 deficiency was associated with markedly lower activity. Fpr1 and Fpr2 double deficiency essentially "phenocopied" the results shown by Fpr2 single deficiency. Therefore, Fpr1 and Fpr2 may possess differential anti–*E. coli* mechanisms, despite their similar activities in mediating chemotaxis and promoting *E. coli* killing. Thus, NET-forming activity joins the list of differential properties for Fpr1 and Fpr2, which also includes ligand specificity and affinity, cell type-specific signaling pathways, and a role in colon crypt development (18). These observations warrant further studies of the similarities and differences for the two receptors in various disease models, especially those related to human diseases.

Fpr-dependent rapid neutrophil infiltration in vivo in response to *E. coli*

To examine the capacity of Fprs to mediate host responses to *E. coli* infection, live bacteria were injected i.v. into the tail vein of mice. The injection resulted in rapid neutrophil accumulation in mouse liver, which reached maximum at 4 h after injection in WT mice (Fig. 6A), with significant reduction after 5 h (data not shown). The recruitment of neutrophils was markedly reduced in the livers of both Fpr1 and Fpr2 single–deficient mice. In FPR1/2 double deficient mouse liver, neutrophil infiltration was almost absent (Fig. 6B, 6C). Thus, Fprs are required for neutrophil accumulation in *E. coli*–infected mouse liver.

To further verify the capacity of Fprs to mediate neutrophil recruitment by *E. coli* in vivo, we i.p. injected FITC-labeled heat-deactivated *E. coli* in WT mice. There was a rapid neutrophil accumulation in mouse peritoneal cavity with the highest level at 3 h after bacterial injection (Fig. 7A, upper-left quadrant). Table I shows a significantly increased neutrophil exudation in the peritoneal cavity of WT mice compared with mice injected with PBS. Both Fpr1 or Fpr2 single deficiency resulted in a marked decrease in *E. coli*–induced neutrophil exudation in the mouse abdominal cavity. Fpr1 and Fpr2 double deficiency was associated with further decreased neutrophil accumulation in the abdominal cavity after *E. coli* injection. The reduced exudation of neutrophils into the peritoneal cavity of Fpr-deficient mice was associated with reduced phagocytosis of FITC-labeled *E. coli* by the cells (Fig. 7B, upper-right quadrant; Table I). These results demonstrate the essential role of Fprs in mediating neutrophil recruitment at *E. coli*–infected sites.

It is worth noting that the phagocytic capability of Fpr-deficient neutrophils appears not to be substantially affected, as demonstrated by similar proportions of neutrophils with phagocytosed *E. coli* recovered from exudates of all mouse strains (Table I). This is consistent with results shown in Fig. 4A, in which some differences in the proportion

and neutrophils containing *E. coli* were observed only at early phases (15–45 min) of phagocytosis experiments. However, despite this, Fpr-deficient neutrophils do show reduced killing of phagocytosed bacteria (Fig. 4B).

To examine the potential involvement of chemokines in neutrophil exudation in the peritoneal cavity injected with *E. coli*, we measured Cxcl1 and Cxcl2, two neutrophil-specific chemokines, in the peritoneal exudates of *E. coli*–infected WT mice. Despite rapid infiltration of neutrophils at 3 h after *E. coli* injection, the production of Cxcl1 and Cxcl2 was minimal at 3 h and reached maximum at 8 h when neutrophil exudation was decreased (Table II). Mice infected with reduced doses of *E. coli* did not show any increase in the production of Cxcl1 and Cxcl2 (data not shown). We also measured the release of LTB4, which is produced at sites of acute inflammation, including as an exosome constituent released by fMLF-stimulated neutrophils (19). As shown in Table II, high concentrations of LTB4 was detected in peritoneal exudates in response to *E. coli* infection. However, the highest concentration of LTB4 appeared after the time when the number of infiltrating neutrophils had already peaked. Reduced bacterial dosage also did not induce higher levels of LTB4 in the peritoneal cavity (data not shown). Therefore, the “rapid wave” of neutrophil infiltration in *E. coli*–infected mice is dependent on Fprs but not on at least some of the major-known neutrophil-specific chemokines.

Increased mortality in Fpr-deficient mice postinfection with a virulent *E. coli* clinical isolate

To test whether Fprs are also involved in host defense against pathogenic *E. coli* infection, we compared the susceptibility of $Fpr1^{-/-}$ and $Fpr1^{+/+}$ mice to infection with a virulent *E. coli* clinical isolate obtained from patient blood at the National Institutes of Health Clinical Center. We injected 10^6 CFUs of the organism i.p., the LD_{50}, to be able to detect both beneficial and harmful effects of Fpr deficiency on the outcome postinfection. $Fpr1^{-/-}$ mice exhibited a markedly higher rate of mortality compared with $Fpr1^{+/+}$ littermates, 95 versus 60%, respectively (Fig. 8A). The increased mortality of $Fpr1^{-/-}$ mice was associated with increased bacterial burden (Fig. 8B). To test whether the increased mortality correlated with Fpr1-mediated neutrophil migration to bacterial products, we collected filtrates of the bacteria cultured for various durations and performed in vitro chemotaxis assays with neutrophils isolated from $Fpr1^{-/-}$ and $Fpr1^{+/+}$ mice. The results showed significantly decreased migration of $Fpr1^{-/-}$ neutrophils compared with $Fpr1^{+/+}$ neutrophils (Supplemental Fig. 1). Consistent with this, we found significantly fewer neutrophils accumulated in the peritoneal cavity in $Fpr1^{-/-}$ mice compared with WT littermates 3 h after *E. coli* infection (Fig. 8C, 8D).

Compared with WT littermates, survival after *E. coli* challenge was also decreased in Fpr2 knockout mice and, to a similar degree, in Fpr1 knockout mice. The two receptors appeared to govern this phenotype in a codominant manner because survival after *E. coli* infection in Fpr1/2 double knockout mice were approximately the same as for Fpr1 and Fpr2 single knockout mice (Fig. 9). The challenge inoculum was extensively washed before injection to reduce any contaminating virulence factors that might artifactually influence the results. In particular, the results in Fig. 9 show that 80% of WT mice survived i.p. infection of *E. coli* after 72 h, whereas all Fpr-deficient mice survived at a rate of <50%.

Discussion

The innate immune system provides the first-line defense against invading microorganisms and endogenous danger signals by activating myeloid cells, in particular, neutrophils that initiate inflammation, microbial clearance, and tissue repair. The invading pathogens are recognized by PRRs such as TLRs on host cells that interact with pathogen-associated molecular patterns (PAMPs) and damage-associated molecular patterns. The best known PAMP derived from *E. coli* is LPS, which interacts with TLR4 on host cells and triggers a cascade of signaling events associated with a plethora of pathophysiological responses (20). In innate immune cells in mammals, activation of TLR4 and adaptor proteins increases phagocytoses and release of bactericidal mediators. However, over activation of TLR4 by LPS may result in a cytokine storm associated with septic shock fatal to the host. TLR4 activation by LPS also causes accumulation of innate immune cells at the site of infection, mostly via induction of chemokines that are either monocyte or neutrophil specific and secreted by host cells. However, *E. coli* as a Gram-negative bacterium has long been known to release formylated peptides (9), which activate specific phagocyte receptors, namely the FPRs.

FPRs are a family of chemoattractant GPCRs that include FPR1, FPR2, and FPR3 in humans and a nine-gene family in mice, of which Fpr1 and Fpr2 have been best characterized functionally. FPRs interact with a number of microbial and host-derived agonists, among which *E. coli* produced fMLF, which is one of the most potent to elicit signaling events leading to myeloid cell migration, mediator release, and increased phagocytosis (21). Recent discoveries with genetically engineered mice with deletion of one or two Fprs have greatly expanded the scope of these receptors in host defense including step-wise trafficking of myeloid cells in host responses to bacterial infection, tissue injury, and wound healing (10, 22). Recognition of bacterial chemotactic peptides positions these receptors as a potential early warning system on phagocytes for bacterial infection. The first in vivo evidence of Fpr1 involvement in host resistance to bacterial infection was demonstrated by the observation in which Fpr1-deficient mice showed significantly reduced resistance to infection by *Listeria monocytogene*s (15), an opportunistic pathogen that infects with a high mortality of immunocompromised individuals. Fpr1 and Fpr2 were subsequently both found to be critical for anti-*Listeria* host defense by mediating rapid neutrophil accumulation at the sites of infection in response to *Listeria*-derived chemotactic peptides (14), which precedes the production of neutrophil-specific chemokines occurring in a later phase of infection (14). Our findings in mouse models of bacterial infection are in accordance with earlier evidence obtained in patients in which individuals with “loss of function mutations” in FPR1 were more susceptible to juvenile periodontitis caused by bacteria infection (23). Therefore, FPRs in both human and mice play an important role in controlling microbial infection.

Our current study extends the importance of both Fpr1 and Fpr2 to host defense against lethal *E. coli* infection. The mechanism appears to involve both receptors in neutrophil accumulation, bacterial phagocytosis, and intracellular killing through activation of the NADPH oxidase. Nevertheless, observations with mouse models should be interpreted with caution when extrapolating to humans. For instance, human patients with Chronic

Granulomatous Disease with absent or very low reactive oxygen species production due to mutations in the NADPH oxidase complex do not suffer from infection caused by *E. coli*, but by other microorganisms, such as *Staphylococcus aureus*. Therefore, more in-depth studies are warranted to elucidate the mechanistic basis of bacterial killing that may differ in human versus mouse models (24).

Although the neutrophil-specific chemokines Cxcl1 and Cxcl2 have been implicated in inducing neutrophil infiltration following TLR-mediated proinflammatory cascades (25–30), and were detected in mouse liver after *Listeria* infection (14), we demonstrate, in this study, that in normal mice, neutrophil accumulation in the abdominal cavity of *E. coli*–infected mice reaches a maximal level at 3 h, which significantly precedes the production of Cxcl1 and Cxcl2 as well as LTB4 in the model. Therefore, neutrophil Fprs appear to be critical for the early recruitment of neutrophils in an *E. coli*–infected site. FPRs are also reported to mediate neutrophil recruitment in other infection models presumably by recognizing a broader range of chemotactic PAMPs (10). Although *E. coli* represents a minor fraction of the normal gut microbiota (31), a decrease in host immunity (for example, in chemotherapy patients developing severe neutropenia) may cause marked expansion and infection resulting in lethal sepsis.

Our results approach closing the circle begun in the 1970s by Schiffmann et al. (12) who first discovered that synthetic short formylated peptides are neutrophil-chemotactic factors. This early work was based on the knowledge that bacterial protein synthesis is initiated by *N*-formylmethionine and that bacterial culture supernatants contain neutrophil chemotactic factors. Finding multiple FPRs was a surprise (8–10). During the past decade, major progress has been achieved thanks to global efforts to delineate the specific pathophysiological role of FPRs (Fprs).

Both Fprs are active participants in host defense against *E. coli* infection as shown in the current study, but with possible differences in the mechanism. Consistent with this, Fpr1 and Fpr2 have overlapping but distinct ligand specificity and affinity, with Fpr2 being more promiscuous than Fpr1 for recognition of host-derived non–*N*-formylated agonists associated with proinflammatory responses (9, 10, 21). Moreover, the two receptors, both in humans and mice, couple to common but also distinct signaling pathways, as documented in hematopoietic versus hematopoietic cell types expressing the receptors, which may account for differences in their biological roles. This notion was supported by our current observations in neutrophils in which Fpr2 coupled strongly and Fpr1 coupled weakly to NET formation in response to *E. coli*, despite the similar capacity of the two receptors to limit *E. coli* infection.

In this context, it is worth noting that although Fpr1 and 2 have both been reported to possess protumorigenic activity by mediating tumor cell proliferation and invasion (10), Fpr2 has also been reported to promote M1 polarization of macrophages in a mouse tumor transplantation model (32) that supported antitumor host defense. But this capacity of Fpr2 may be a “double-edged sword” because M1 polarization–associated proinflammatory responses worsen the pathologic changes of diabetic retinopathy in the eye (33) as well as the obesity and insulin resistance observed in mice fed a high fat diet (34).

The development of Fpr-targeted mice was critical for dissecting the relative contributions of Fpr1 and Fpr2 to neutrophil responses and mouse susceptibility to *E. coli* and will enable future studies designed to interrogate other roles for the receptors in health and diseases.

Supplementary Material

Refer to Web version on PubMed Central for supplementary material.

Acknowledgments

We thank Dr. Joost J. Oppenheim for critically reviewing the manuscript and Timothy Back for assistance in animal experiments. The secretarial assistance by Cheri A. Rhoderick is also appreciated.

This work was supported by federal funds from the National Cancer Institute (NCI), National Institutes of Health (NIH) under Contract HSN261200800001E and by the Intramural Research Programs of the NCI and the National Institute of Allergy and Infectious Diseases, NIH. M.Z. was also supported in part by National Natural Science Foundation of China Grant 81873842, Shandong University, Jinan, People's Republic of China.

Abbreviations used in this article:

BM	bone marrow
FPR	Fpr, formyl peptide receptor
GPCR	G protein–coupled receptor
NET	neutrophil extracellular trap
PAMP	pathogen-associated molecular pattern
PMN	polymorphonuclear neutrophil
PRR	pattern recognition receptor
WT	wild-type

References

1. Bentley R, and Meganathan R. 1982. Biosynthesis of vitamin K (menaquinone) in bacteria. Microbiol. Rev46: 241–280. [PubMed: 6127606]
2. Kawai T, and Akira S. 2005. Pathogen recognition with toll-like receptors. Curr. Opin. Immunol17: 338–344. [PubMed: 15950447]
3. Miller SI, Ernst RK, and Bader MW. 2005. LPS, TLR4 and infectious disease diversity. Nat. Rev. Microbiol3: 36–46. [PubMed: 15608698]
4. Qureshi ST, Larivière L, Leveque G, Clermont S, Moore KJ, Gros P, and Malo D. 1999. Endotoxin-tolerant mice have mutations in toll-like receptor 4 (Tlr4). [Published erratum appears in 1999 J. Exp. Med. 189: following 1518.]J. Exp. Med189: 615–625. [PubMed: 9989976]
5. Haruta Y, Koarada S, Tada Y, Mitamura M, Ohta A, Fukuoka M, Hayashi S, and Nagasawa K. 2007. High expression of toll-like receptor 4 on CD14+ monocytes in acute infectious diseases. Scand. J. Infect. Dis39: 577–583. [PubMed: 17577821]
6. Foster N, Lea SR, Preshaw PM, and Taylor JJ. 2007. Pivotal advance: vasoactive intestinal peptide inhibits up-regulation of human monocyte TLR2 and TLR4 by LPS and differentiation of monocytes to macrophages. J. Leukoc. Biol81: 893–903. [PubMed: 16973891]

7. Xiong Z, Song J, Yan Y, Huang Y, Cowan A, Wang H, and Yang XF. 2008. Higher expression of Bax in regulatory T cells increases vascular inflammation. Front. Biosci13: 7143–7155. [PubMed: 18508723]
8. Mei S, Liu Y, Wu X, He Q, Min S, Li L, Zhang Y, and Yang R. 2016. TNF-α-mediated microRNA-136 induces differentiation of myeloid cells by targeting NFIA. J. Leukoc. Biol99: 301–310. [PubMed: 26329426]
9. Le Y, Murphy PM, and Wang JM. 2002. Formyl-peptide receptors revisited. Trends Immunol. 23: 541–548. [PubMed: 12401407]
10. Chen K, Bao Z, Gong W, Tang P, Yoshimura T, and Wang JM. 2017. Regulation of inflammation by members of the formyl-peptide receptor family. J. Autoimmun85: 64–77. [PubMed: 28689639]
11. Chadwick VS, Mellor DM, Myers DB, Selden AC, Keshavarzian A, Broom MF, and Hobson CH. 1988. Production of peptides inducing chemotaxis and lysosomal enzyme release in human neutrophils by intestinal bacteria in vitro and in vivo. Scand. J. Gastroenterol23: 121–128. [PubMed: 3278364]
12. Schiffmann E, Corcoran BA, and Wahl SM. 1975. N-formylmethionyl peptides as chemoattractants for leucocytes. Proc. Natl. Acad. Sci. USA72: 1059–1062. [PubMed: 1093163]
13. Krepel SA, and Wang JM. 2019. Chemotactic ligands that activate G-protein-coupled formylpeptide receptors. Int. J. Mol. Sci20: 3426.
14. Liu M, Chen K, Yoshimura T, Liu Y, Gong W, Le Y, Gao JL, Zhao J, Wang JM, and Wang A. 2014. Formylpeptide receptors mediate rapid neutrophil mobilization to accelerate wound healing. [Published erratum appears in 2014 PLoS One 9: e99541.]PLoS One9: e90613. [PubMed: 24603667]
15. Gao JL, Lee EJ, and Murphy PM. 1999. Impaired antibacterial host defense in mice lacking the N-formylpeptide receptor. J. Exp. Med189: 657–662. [PubMed: 9989980]
16. Chen K, Le Y, Liu Y, Gong W, Ying G, Huang J, Yoshimura T, Tessarollo L, and Wang JM. 2010. A critical role for the g protein-coupled receptor mFPR2 in airway inflammation and immune responses. J. Immunol184: 3331–3335. [PubMed: 20200280]
17. Altschul SF, Madden TL, Schäffer AA, Zhang J, Zhang Z, Miller W, and Lipman DJ. 1997. Gapped BLAST and PSI-BLAST: a new generation of protein database search programs. Nucleic Acids Res. 25: 3389–3402. [PubMed: 9254694]
18. Chen K, Liu M, Liu Y, Yoshimura T, Shen W, Le Y, Durum S, Gong W, Wang C, Gao JL, et al.2013. Formylpeptide receptor-2 contributes to colonic epithelial homeostasis, inflammation, and tumorigenesis. J. Clin. Invest123: 1694–1704. [PubMed: 23454745]
19. Majumdar R, Tavakoli Tameh A, and Parent CA. 2016. Exosomes mediate LTB4 release during neutrophil chemotaxis. PLoS Biol. 14: e1002336. [PubMed: 26741884]
20. Chen K, Bao Z, Tang P, Gong W, Yoshimura T, and Wang JM. 2018. Chemokines in homeostasis and diseases. Cell. Mol. Immunol15: 324–334. [PubMed: 29375126]
21. Ye RD, Boulay F, Wang JM, Dahlgren C, Gerard C, Parmentier M, Serhan CN, and Murphy PM. 2009. International Union of Basic and Clinical Pharmacology. LXXIII. Nomenclature for the formyl peptide receptor (FPR) family. Pharmacol. Rev61: 119–161. [PubMed: 19498085]
22. McDonald B, Pittman K, Menezes GB, Hirota SA, Slaba I, Waterhouse CC, Beck PL, Muruve DA, and Kubes P. 2010. Intravascular danger signals guide neutrophils to sites of sterile inflammation. Science330: 362–366. [PubMed: 20947763]
23. Perez HD, Kelly E, Elfman F, Armitage G, and Winkler J. 1991. Defective polymorphonuclear leukocyte formyl peptide receptor(s) in juvenile periodontitis. J. Clin. Invest87: 971–976. [PubMed: 1999504]
24. Roos D, and de Boer M. 2014. Molecular diagnosis of chronic granulomatous disease. Clin. Exp. Immunol175: 139–149. [PubMed: 24016250]
25. Chapman RW, Minnicozzi M, Celly CS, Phillips JE, Kung TT, Hipkin RW, Fan X, Rindgen D, Deno G, Bond R, et al.2007. A novel, orally active CXCR1/2 receptor antagonist, Sch527123, inhibits neutrophil recruitment, mucus production, and goblet cell hyperplasia in animal models of pulmonary inflammation. J. Pharmacol. Exp. Ther322: 486–493. [PubMed: 17496165]

26. Rose JJ, Foley JF, Murphy PM, and Venkatesan S. 2004. On the mechanism and significance of ligand-induced internalization of human neutrophil chemokine receptors CXCR1 and CXCR2. J. Biol. Chem279: 24372–24386. [PubMed: 15028716]
27. Chintakuntlawar AV, and Chodosh J. 2009. Chemokine CXCL1/KC and its receptor CXCR2 are responsible for neutrophil chemotaxis in adenoviral keratitis. J. Interferon Cytokine Res29: 657–666. [PubMed: 19642907]
28. Zhang L, Ran L, Garcia GE, Wang XH, Han S, Du J, and Mitch WE. 2009. Chemokine CXCL16 regulates neutrophil and macrophage infiltration into injured muscle, promoting muscle regeneration. Am. J. Pathol175: 2518–2527. [PubMed: 19893053]
29. Burdon PC, Martin C, and Rankin SM. 2005. The CXC chemokine MIP-2 stimulates neutrophil mobilization from the rat bone marrow in a CD49d-dependent manner. Blood105: 2543–2548. [PubMed: 15542579]
30. Monson KM, Dowlatshahi S, and Crockett ET. 2007. CXC-chemokine regulation and neutrophil trafficking in hepatic ischemia-reperfusion injury in P-selectin/ICAM-1 deficient mice. J. Inflamm. (Lond.)4: 11. [PubMed: 17524141]
31. Bailey JK, Pinyon JL, Anantham S, and Hall RM. 2010. Commensal *Escherichia coli* of healthy humans: a reservoir for antibiotic-resistance determinants. J. Med. Microbiol59: 1331–1339. [PubMed: 20671087]
32. Liu Y, Chen K, Wang C, Gong W, Yoshimura T, Liu M, and Wang JM. 2013. Cell surface receptor FPR2 promotes antitumor host defense by limiting M2 polarization of macrophages. Cancer Res. 73: 550–560. [PubMed: 23139214]
33. Yu Y, Bao Z, Wang X, Gong W, Chen H, Guan H, Le Y, Su S, Chen K, and Wang JM. 2017. The G-protein-coupled chemoattractant receptor Fpr2 exacerbates high glucose-mediated proinflammatory responses of Müller glial cells. Front. Immunol8: 1852. [PubMed: 29312335]
34. Chen X, Zhuo S, Zhu T, Yao P, Yang M, Mei H, Li N, Ma F, Wang JM, Chen S, et al.2019. Fpr2 deficiency alleviates diet-induced insulin resistance through reducing body weight gain and inhibiting inflammation mediated by macrophage chemotaxis and M1 polarization. Diabetes68: 1130–1142. [PubMed: 30862681]

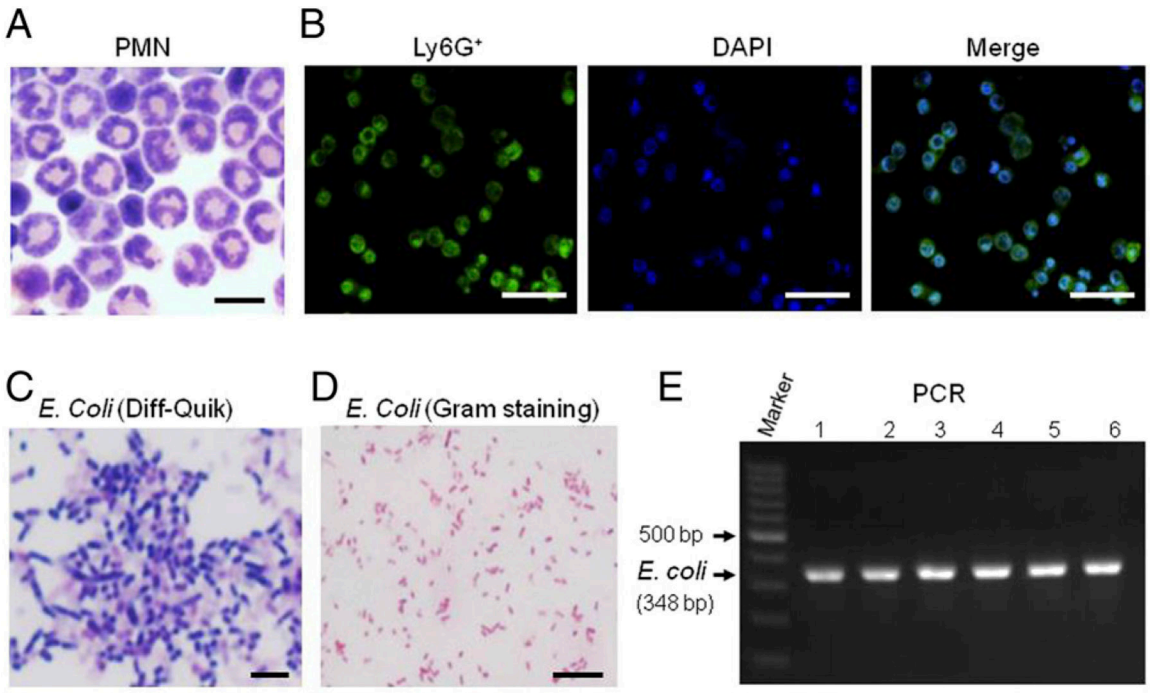

FIGURE 1.

Characterization of mouse neutrophils and *E. coli*. (**A**) Representative image to show neutrophils. Neutrophils were isolated from mouse BM after culture with G-CSF for 24 h. Cell smears were stained with Diff-Quik, showing polymorphic nuclei. The experiment was repeated three times ($n = 3–5$). Scale bar, 10 μm. (**B**) Representative image to show $Ly6G^+$ neutrophils. Cells labeled with neutrophil-specific Ab Ly6G showing more than 85% purity. The experiment was repeated three times ($n = 3–5$). Scale bar, 10 μm. (**C**) Representative image to show *E. coli*. *E. coli* was isolated from the colon of WT mice after DSS intake for 5 d and bacterial smears were stained with Diff-Quik, showing rod-shaped organisms. The experiment was repeated three times. Scale bar, 20 μm. (**D**) Representative image to show Gram negative *E. coli*. *E. coli* smear was stained with Gram Stain Kit and the bacteria were Gram negative. The experiment was repeated three times. Scale bar, 10 μm. (**E**) Representative image to show PCR for *E. coli*. Colonies of *E. coli* were expanded in LB Broth for 24 h for PCR analysis of extracted DNA using *E. coli*-specific primers. PCR products were resolved on 1.5% agarose gel by electrophoresis and visualized after ethidium bromide staining, the experiment was repeated three times. *E. coli* samples are from six colonies.

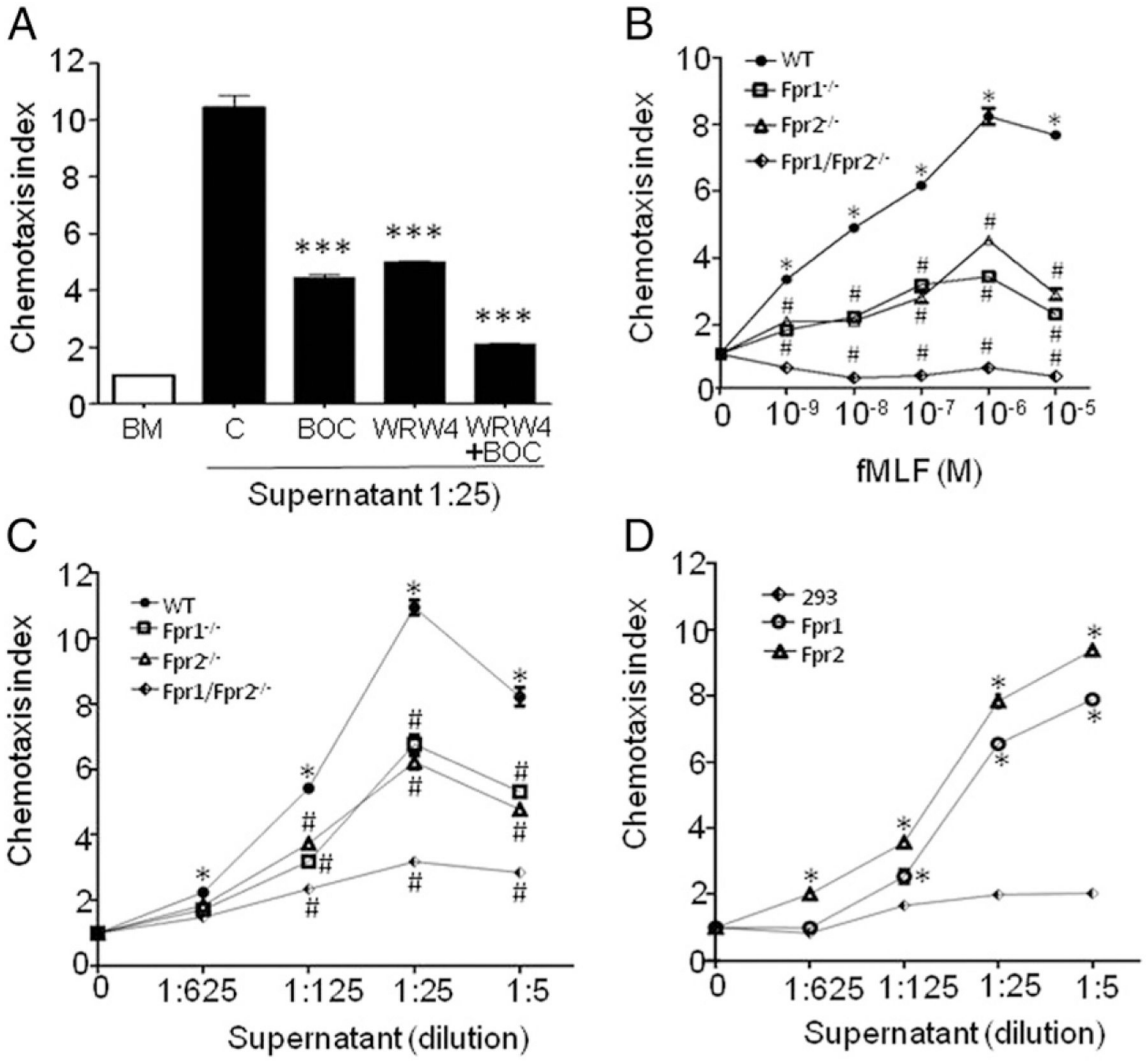

FIGURE 2.

Involvement of Fprs in sensing *E. coli*–derived chemotactic signals. (**A**) Chemotactic response of mouse neutrophils to *E. coli* supernatant. Fpr1 antagonist BOC-MLF was tested at 5 ng/ml; Fpr2 antagonist WRW4 was tested at 10 ng/ml. The experiment was repeated three times (n = 3–5 mice per group). ***$p < 0.001$ compared with no antagonist. (**B**) Chemotactic activity of fMLF for mouse neutrophils. *$p < 0.05$ compared with medium control. $^{\#}p < 0.05$ compared with WT neutrophils. The experiment was repeated three times (n = 3–5 mice per group). (**C**) Migration of mouse neutrophils deficient in Fprs to *E. coli* supernatant. The experiment was repeated three times (n = 3–5 mice per group). *$p < 0.05$ compared with medium control. $^{\#}p < 0.05$ compared with WT neutrophils. (**D**) Chemotactic activity of *E. coli* supernatant for HEK293 cells transfected with Fprs. *$p < 0.05$ compared with medium control. Parental 293 cells failed to migrate in response to *E. coli* supernatants. The experiment was repeated three times.

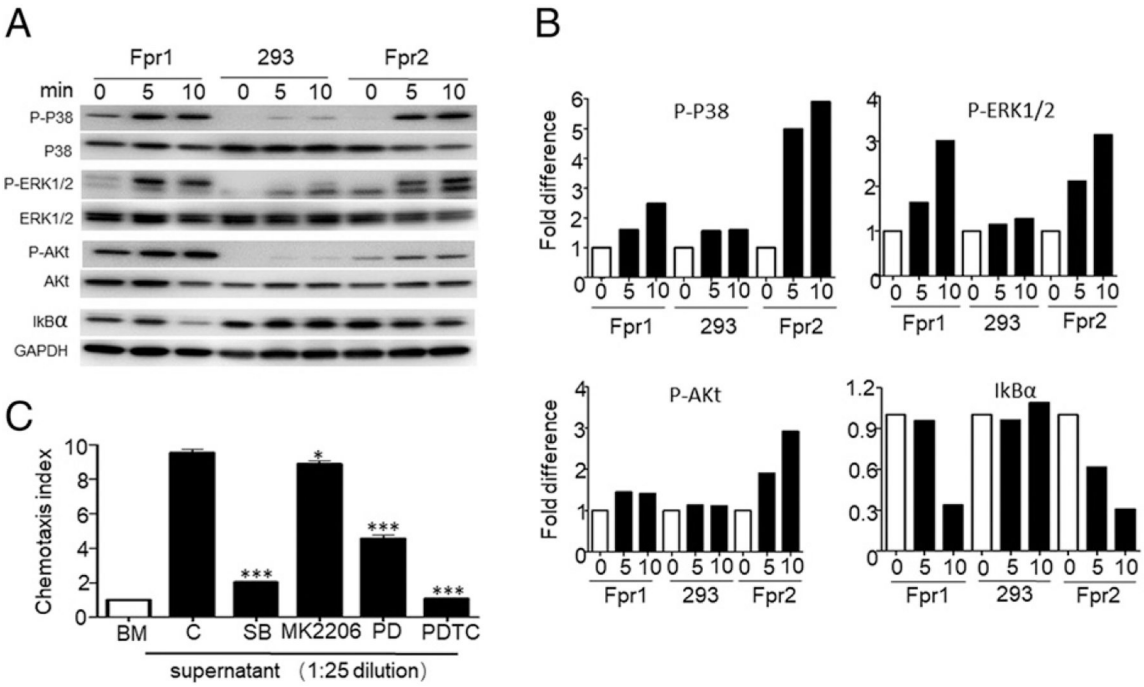

FIGURE 3.

Activation of mouse Fprs by *E. coli* supernatant. (**A**) The response of Fpr1 and Fpr2 transfected HEK293 cells to *E. coli* supernatant. Cells were stimulated by *E. coli* supernatant at a 1:25 dilution. The indicated phosphoproteins were analyzed 5 and 10 min after stimulation. The experiment was repeated three times. (**B**) Representative result to show the semiquantitative analysis of p-p38, ERK1/2, Akt, and activated IkBα. The experiment was repeated three times. (**C**) Representative result to show the reduced *E. coli* supernatant–induced neutrophil migration by inhibitors of p38 (SB203580, 10 μM), ERK1/2 (PD98059, 10 μM), Akt (Mk2206, 20 μM), and IkBα (PDTC, 10 μM). The experiment was repeated three times. *$p < 0.05$, ***$p < 0.001$.

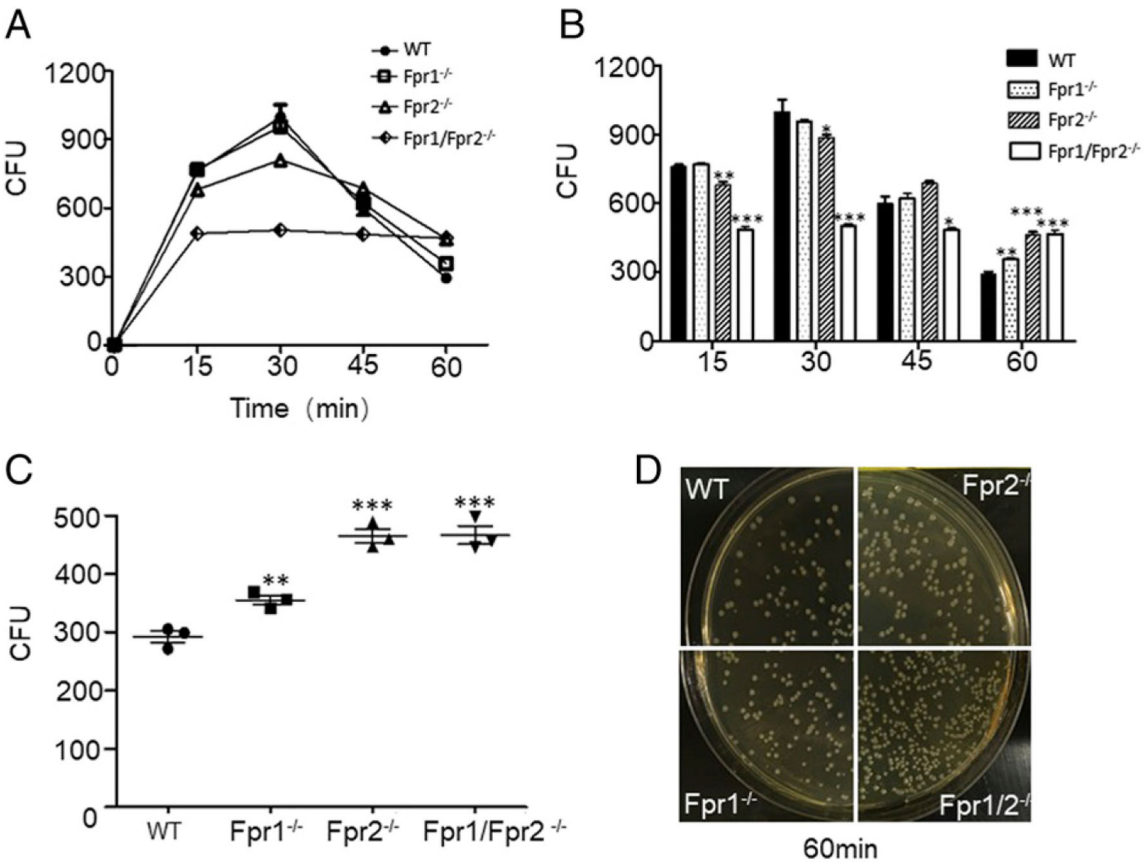

FIGURE 4.

Fpr-dependent *E. coli* phagocytosis and killing by mouse neutrophils. (**A**) Endocytosis capacity of neutrophils. Mouse neutrophils were incubated with 10-fold live *E. coli* for 15, 30, 45, and 60 min at 37°C. Nonphagocytosed bacteria were removed by washing. The cells were then lysed to detect *E. coli* CFUs after 24 h culture on agar. The experiment was repeated three times (n = 3–5 mice per group). (**B**) Decreased phagocytosis of *E. coli* by neutrophils from Fpr single and double deficient mice as comparative with cells from WT mice. *$p < 0.05$, **$p < 0.01$, ***$p < 0.001$. The experiment was repeated three times (n = 3–5 mice per group). (**C**) The killing capacity shown by neutrophils. Significantly increased *E. coli* CFUs detected in lysed Fpr-deficient mouse neutrophils after coculture with *E. coli* as compared with WT neutrophil. **$p < 0.01$, ***$p < 0.001$. The experiment was repeated three times (n = 3–5 mice per group). (**D**) Lysates of mouse neutrophils incubated with 10-fold live *E. coli* for 1 h showing *E. coli* CFUs after 24 h culture on agar. Increased *E. coli* CFUs were detected in lysed Fpr-deficient mouse neutrophils after coculture for 60 min with *E. coli* as compared with WT neutrophils. The experiment was repeated three times (n = 3–5 mice per group).

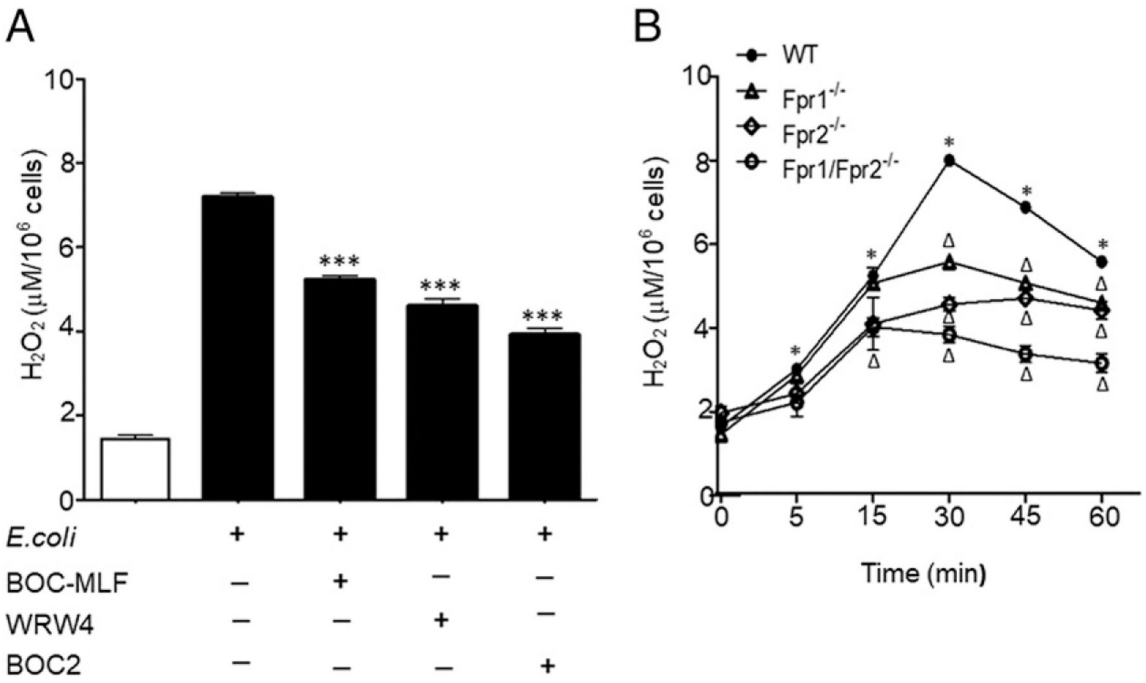

FIGURE 5.

Production of H_2O_2 by neutrophils in response to *E. coli*. (**A**) Neutrophils derived from WT mouse BM were incubated with the Fpr antagonists Boc-MLF (5 ng/ml), WRW4 (10 ng/ml), or BOC2 (10 ng/ml) for 30 min before measurement for production of H_2O_2 postinfection by *E. coli*. ***$p < 0.001$. The experiment was repeated three times ($n = 3–5$ mice per group). (**B**) Neutrophils derived from WT mouse BM, showing increased release of H_2O_2 after *E. coli* infection. *$p < 0.05$ compared with cells at time zero, $^{\Delta}p < 0.05$. The experiment was repeated three times ($n = 3–5$ mice per group).

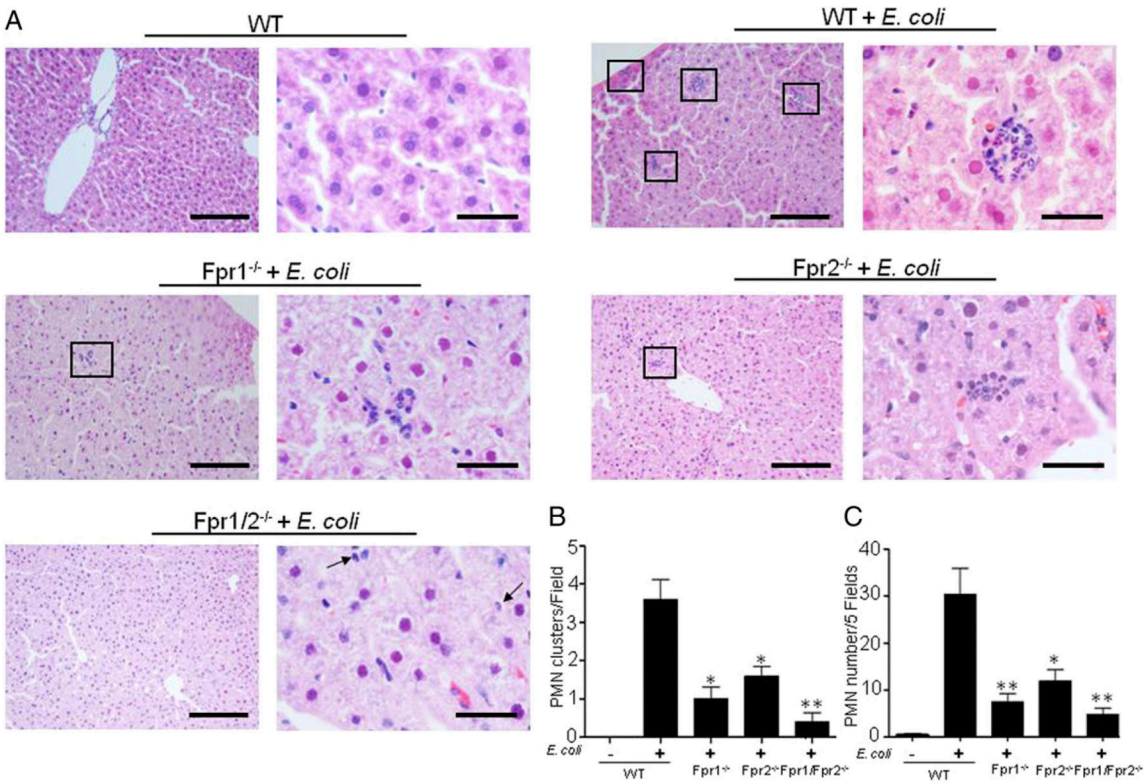

FIGURE 6.

Neutrophil infiltration in mouse liver after i.v. injection of *E. coli*. Mice were injected i.v. through the tail vein with 5×10^4 CFUs of *E. coli*. The liver was harvested at 4 h after bacterial injection, fixed, paraffin embedded, sectioned in 5-μm slices, stained with H&E, and examined under light microscopy. (**A**) Decreased neutrophil accumulation in the liver of Fpr-deficient mice compared with the liver of WT mice. Left panel for each group: scale bar, 100 μm. Right panel for each group: scale bar, 10 μm ($n = 5$ mice per group). The experiment was repeated three times. (**B**) Significantly reduced number of neutrophil clusters in the liver of Fpr-deficient mice compared with WT mice (*$p < 0.05$, **$p < 0.01$). (**C**) Decreased neutrophil number in single-cell clusters in the liver of Fpr-deficient mice compared with WT mice (**$p < 0.01$).

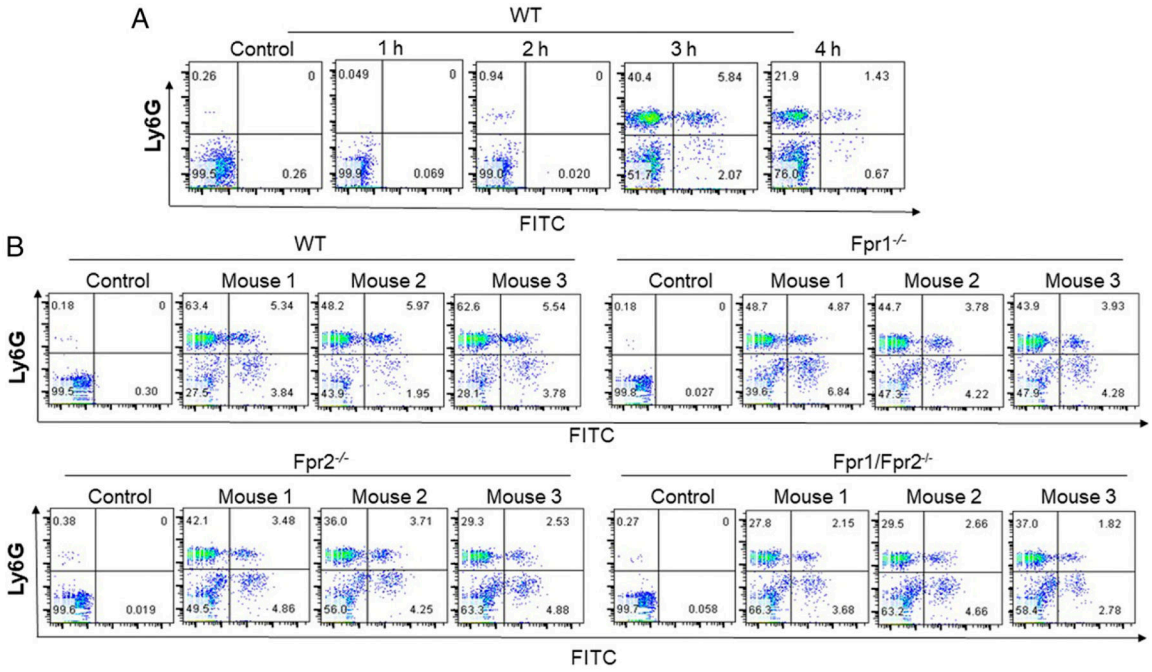

FIGURE 7.

PMN accumulation in mouse peritoneal cavity after inoculation of heat-inactivated *E. coli*. (**A**) FITC-labeled heat-inactivated *E. coli* was injected into the peritoneal cavity of WT mice. PBS injection was used as control. Cells in mouse peritoneal cavity were collected 1, 2, 3, and 4 h after injection. FACS analysis demonstrates optimal neutrophil accumulation in mouse peritoneal cavity at 3 h after injection, which also show optimal bacteria phagocytosis by neutrophils. (**B**) Upper-left quadrant: the ratio of neutrophils labeled by LYG6. Upper-right quadrant: The ratio of neutrophils containing phagocytosed *E. coli*. Lower-left quadrant: Ly6G negative cells in the peritoneal cavity. Lower-right quadrant: *E. coli*. Results from three mice deficient in Fpr1, Fpr2, or both are shown with reduced exudation of total neutrophils with lower levels of phagocytosis of FITC-labeled *E. coli* as compared to WT mice (quantitative results are shown in Table I). The experiment was repeated three times (n = 4–5 mice per group).

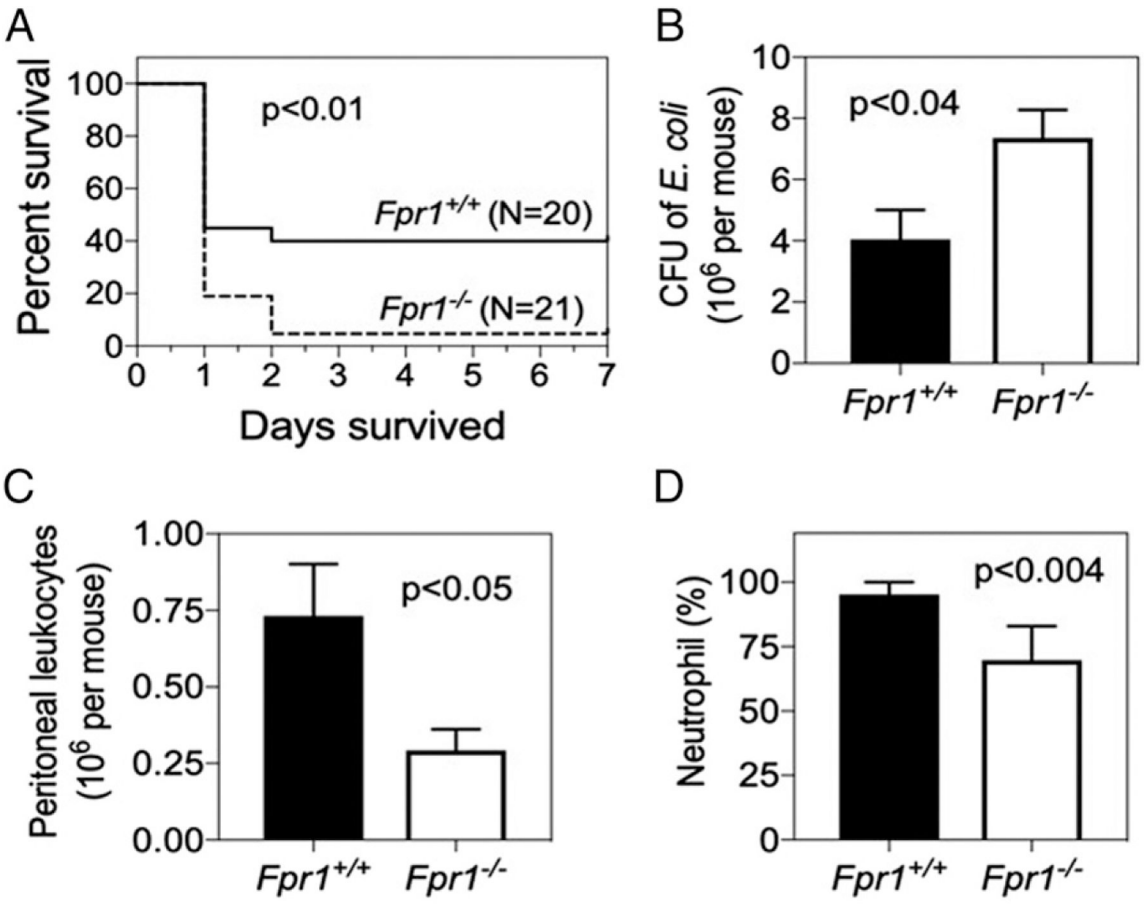

FIGURE 8.

Increased mortality in *Fpr1*$^{-/-}$ mice postinfection with a clinical isolate of *E. coli*. (**A**) Mortality. Male *Fpr1*$^{+/+}$ or *Fpr1*$^{-/-}$ mice were injected with 10^6 CFUs in the peritoneal cavity. The numbers of mice (N) are indicated in the figure. Results are from a single experiment and are representative of three separate experiments with a consistent pattern. (**B**) Bacterial burden. Mice were injected with 3×10^6 CFUs of *E. coli* in the peritoneal cavity and euthanized 3 h after injection. The peritoneal cavity was flushed with 10 ml of PBS. *E. coli* CFU per mouse was analyzed by plating serial dilutions of flushed peritoneal fluid on LB agar plates. (**C** and **D**) Neutrophil accumulation. Mice were injected with 3×10^6 CFUs in the peritoneal cavity and euthanized 3 h after injection. The peritoneal cavity was washed with 10 ml of PBS. (C) Total leukocytes collected from the peritoneal cavity. (D) Percent neutrophils. Results are from a single experiment of five animals in each group and are representative of three separate experiments with a consistent pattern (B–D).

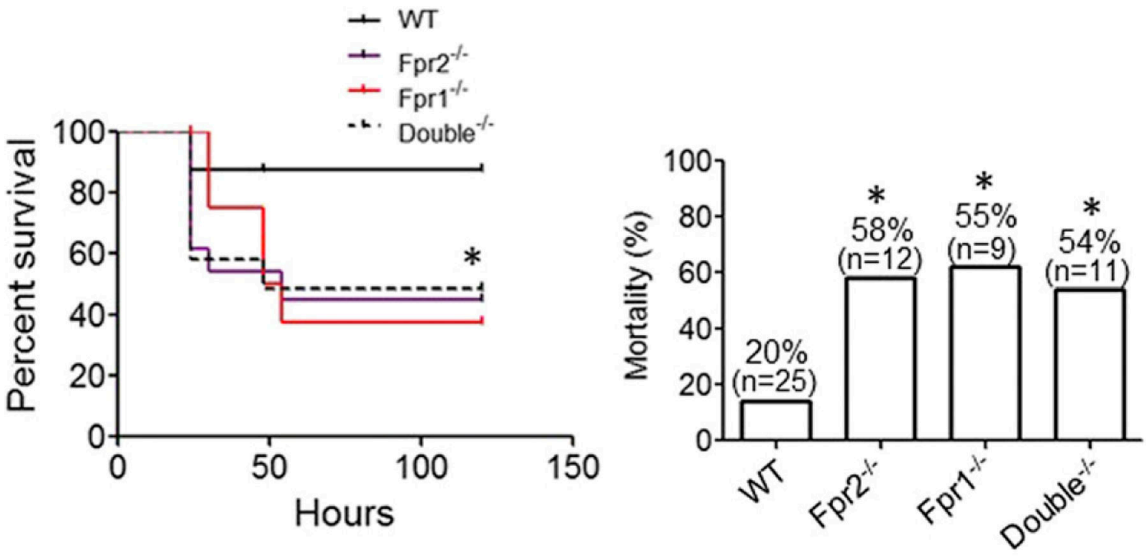

FIGURE 9.

The mortality of mice after i.p injection of a clinical *E. coli* isolate. *E. coli* was grown to log-phase in LB Broth, aliquoted in 1 ml volumes, and stored at −80°C. For experiments, the bacteria were thawed and washed with sterile PBS three times to remove toxins, then were suspended in PBS. WT, *Fpr1*$^{-/-}$, *Fpr2*$^{-/-}$, and double$^{-/-}$ mice (male, 6- to 8-wk-old) were i.p. injected with *E. coli* at 10^6 CFUs per mouse. Left panel, Percent survival of mice after *E. coli* injection. Right panel, The mortality of mice. *$p < 0.05$, significantly increased mortality of Fpr-deficient mice as compared with WT mice (log-rank Mantel-Cox [left panel] and Kruskal–Wallis [right panel] tests). Data are the representative from three performed with comparable results.

Table I.

PMN accumulation in mouse peritoneal cavity after inoculation with heat-inactivated *E. coli*[a]

		E. coli Injection		
	PBS Total Cells (10^4)	**Total Cells (10^4)**	**PMN (10^4)**	***E. coli*$^+$ PMN (10^4)**
WT	216 ± 14.4	572 ± 93.7^{**,b}	359.1 ± 8.5	32.1 ± 7.4
Fpr1$^{-/-}$	202 ± 17.5	281 ± 33.6$^{*\Delta\Delta,c}$	140.3 ± 14.4$^{\#\#\#,d}$	11.7 ± 1.2$^{\#\#}$
Fpr2$^{-/-}$	229 ± 34.0	337 ± 76.6$^{\Delta}$	132.1 ± 43.7$^{\#\#\#}$	10.8± 2.7$^{\#\#}$
Fpr1$^{-/-}$/Fpr2$^{-/-}$	206 ± 19.7	255 ± 34.4$^{\Delta\Delta}$	85.8 ± 17.3$^{\#\#\#}$	5.5 ± 0.6$^{\#\#}$

[a]FITC-labeled heat-inactivated *E. coli* was injected into the peritoneal cavity of the indicated strains of mice. PBS was injected as a control. Cells in mouse peritoneal cavity were collected 3 h after injection.

[b]Asterisks denote significantly increased cell number in *E. coli*–injected mouse cavity as compared with mice injected with PBS. *$p < 0.05$, **$p < 0.01$.

[c]Triangles denote significantly reduced total cell number in Fpr-deficient mouse peritoneal cavity as compared with WT mice. $^{\Delta}p < 0.05$, $^{\Delta\Delta}p < 0.01$.

[d]Pound symbols (#) denote significantly reduced number of total neutrophils and neutrophils phagocytosing FITC-labeled *E. coli* in Fpr-deficient mouse peritoneal cavity compared with WT mice. $^{\#\#}p < 0.01$, $^{\#\#\#}p < 0.001$.

Table II.

Production of Cxcl1 and Cxcl2 in mouse peritoneal cavity

	Time (h)[a]				
	1	**3**	**8**	**12**	**24**
Cxcl1 (pg/ml)	0.4 ± 0.4	37.3 ± 7.4 ***,b***	841.2 ± 230.2 ***	3.0 ± 1.0 *	1.3 ± 0.9 *
Cxcl2 (pg/ml)	1.1 ± 0.1	33.2 ± 4.9 ΔΔΔ,c	304.3 ± 71.0 ΔΔΔ	10.2± 2.4 ΔΔ	6.4 ± 2.1 Δ
LTB4 (pg/ml)	3.6 ± 0.4	44.3± 5.8 ###, d	456.6 ± 81.2 ###	202.4± 20.4 ###	110.4 ± 32.1 ###

[a] Peritoneal fluid was collected at 1, 3, 8, 24, and 48 h after i.p. injection of *E. coli.* CxclL1 and Cxcl2 in the peritoneal exudates were measured by U-PLEX assays. LTB4 was measured by an ELISA kit. LTB4 was measured with an LTB4 enzyme-linked immunoassay kit (Cayman Chemical, Ann Arbor, MI) according to the manufacturer's instructions.

[b] Asterisks denote significantly increased Cxcl1 compared with 1 h. *$p < 0.05$, **$p < 0.01$, ***$p < 0.001$.

[c] Triangles denote significantly increased Cxcl2 compared with 1 h. $^{\Delta}p < 0.05$, $^{\Delta\Delta}p < 0.01$, $^{\Delta\Delta\Delta}p < 0.001$.

[d] Pound symbols (#) denote significantly increased LTB4 compared with 1 h. $^{\#\#\#}p < 0.001$.